Cite this: DOI: 10.1039/c0xx00000x

www.rsc.org/xxxxxx

Communication

Hyperbranched Polyester Nanorods with Pyrrolo[2,1-a]isoquinoline End-Groups for Fluorescent Recognition of Fe^{3+}

Qiaorong Han[1*], Yuliang Jiang[1], Can Jin[2], Shanshan Cheng[1], Xiaoxia Wang[1], Xiangyu Wang[1], and Bingxiang Wang[1]*

Received (in XXX, XXX) Xth XXXXXXXXX 20XX, Accepted Xth XXXXXXXXX 20XX

DOI: 10.1039/b000000x

Herein, we reported the synthesis of hyperbranched aromatic-aliphatic co-polyester nanorods HBPE-CICA$_6$ and HBPE-CICA$_2$ by modifing periphery of the second generation hyperbranched polyester (HBPE) with 1-cyano-pyrrolo[2,1-a]isoquinoline-3-carboxylic acid (CICA) groups. Structures of HBPE-CICAs were confirmed by combined studies of fourier transform infrared spectroscopy (FTIR), proton nuclear magnetic resonance (^{1}H NMR), transmission electron microscopy (TEM), atomic force microscopy (AFM) and X-ray diffraction (XRD). The potential application of HBPE-CICAs in ion recognition was investigated, in particular, the HBPE-CICA$_2$, exhibited remarkable selectivity for Fe^{3+}.

Due to the highly branched structures, multitude of available surface groups and improved solubilities compared to their linear analogues, hyperbranched polymers have attracted extensive interests as an unique class of architectural macromolecules during the past decades.[1-4] The controlled internal organization of these architectures in the form of fibers, nanotubes, zigzags, and helices has been modified with well-defined and rigid configurations and conformations.[5] To date, assemblies of hyperbranched polymers can be engineered to obtain supramolecular assemblies with combined or enhanced properties which remains challenging and has only been addressed in a few studies.[6-9]

In particular, hyperbranched polyesters (HBPE), one important class of the hyperbranched polymers family, were widely used for academic research[10-15] and applications in the fields of biology,[16] medicine,[17, 18] pharmacy[19, 20, 21] and electronics.[22] Recently, a variety of molecular designs have been proposed for the fabrication of nanostructured HBPE, which would lead to multifunctional macromolecule materials. Santra, Santimukul and coworkers reported the multifunctional hyperbranched polyester-based nanoparticles and nanocomposites with properties ranging from magnetic, fluorescence, antioxidant.[10] Our group reported novel water-soluble nanoparticles made up of hyperbranched polyester with sulfonic acid end-groups and their anticoagulant effect and cytotoxicity,[23] those nanoparticles showed the spherical morphology. However, there are only a handful of reports on the formation of organized nanorod structures from hyperbranched molecules composed of irregular, random branched fragments with the degree of branching well below that observed for the dendrimer architecture[5, 24-26], since hyperbranched molecules are generally not expected to form regular supramolecular nanorod structures owning to their high polydispersities, irregular architectures, and poorly defined shapes. Moreover, the synthesis of hyperbranched polyester nanorods modified with the heterocyclic nitrogen compounds has been sparsely developed, which provoked us to initiate our present study.

Pyrrolo[2,1-a]isoquinolines derivatives are valuable heterocyclic nitrogen compounds, which have been widely utilized in pharmaceutical chemistry,[27-29] functional materials.[30] Much attention has been focused on diversity-oriented synthesis[31-36] to expand the design of architecture, including heterocycles, populating unexplored “chemical space” to aid the discovery of novel lead compounds.[37-39] Furthermore, N atoms and aromatic nucleus of pyrrolo[2,1-a]isoquinolines derivatives are considered to be efficient hydrogen bond acceptor and π-π stacking units in supramolecular functional polymers with distinctively biological and physical features.

The aim of this study was to design and synthesize a new class of HBPE-CICA nanorods by modifying 1-cyano-pyrrolo[2,1-a]isoquinoline-3-carboxylic acid (CICA) to the second generation of HBPE structure. Because the modified molecules with the presence of CICA tails and residual hydroxyl groups in the flexible core, which might exhibit multiple intermolecular interactions among highly branched molecules, and facilitate their assembly into supramolecular nanorod structures. It is worth to understand the role of amphiphilic balances and the combination of the functional terminal groups during nanorod structures formation in one-pot synthesis. In addition, we expect to investigate the fluorescence diversification of these functionalized HBPE-CICA nanorods in presence of various metal cations to look into their potentials as fluorescence sensors in chemical or biological applications.

The synthetic route of 1-cyano-pyrrolo[2,1-a]isoquinoline-3-carboxylic acid (CICA) in three steps were described in scheme 1 and the synthesis methods were described in scheme S1. The target compound was characterized by IR (Fig. 1), ^{1}H NMR(Fig.

2) and ESI-MS spectra (Fig. S1 in Supporting Information).

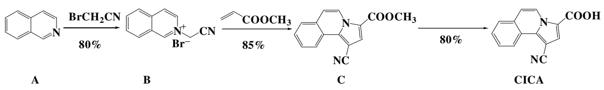

Scheme 1 Synthetic route of CICA

The synthetic routes of HBPE and HBPE-CICA were described as scheme 2 and the synthesis methods were described in scheme S2. The structures of modified hyperbranched polyester HBPE-$CICA_6$ and HBPE-$CICA_2$ were confirmed by FT-IR, ^{1}H NMR and ESI-MS. As shown in Fig. 1, the FT-IR spectra of HBPE-$CICA_6$ and HBPE-$CICA_2$ were found to be quite similar to those of CICA and HBPE. All of them showed similar characteristic peaks of benzene ring at 1617, 1550, 1499 and 1455 cm^{-1}; signals of C=O at 1695 cm^{-1} and 1638 cm^{-1}; signals of -C-O-C- at 1125 cm^{-1}. The characteristic peaks of -CN at 2217 cm^{-1} were obviously observed only for CICA, HBPE-$CICA_6$ and HBPE-$CICA_2$ (blue, black and red curves, respectively), while not exist in unmodified HBPE (green curve).

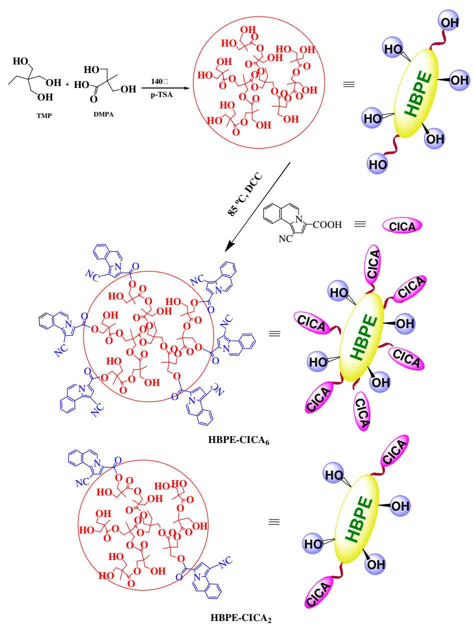

Scheme 2 Synthetic route of HBPE, HBPE-$CICA_6$ and HBPE-$CICA_2$

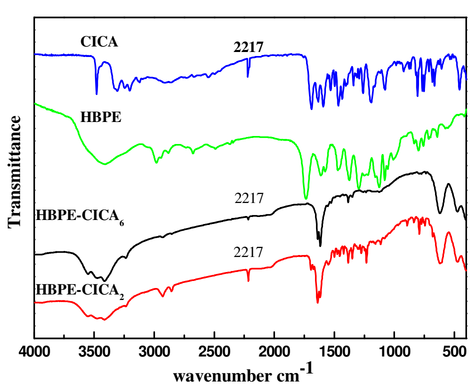

Fig. 1 FTIR spectra of CICA (blue line), HBPE (green line), HBPE-$CICA_6$ (black line) and HBPE-$CICA_2$ (red line)

^{1}H NMR (Fig. 2) spectra was further carried out to confirm the chemical composition of the modified samples. Signals at 7.33-8.73 ppm were attributed to the modified end-groups (CICA). Protons of $R_3CCOOCH_2$ and $ArCOOCH_2$ could be observed at 3.42 and 4.10 ppm, respectively, while those of methyl groups appeard at 0.83–1.75 ppm. Moreover, the CICA grafting of HBPE-$CICA_6$ and HBPE-$CICA_2$ could be calculated by integration ratio of the aromatic protons (**b**) to alphatic protons (**a**) (CH_3- and CH_3CH_2- groups) with the formula ($8S_b/(21S_a)$) were about 50% and 13%, respectively. The ESI-MS(m/z) of HBPE-$CICA_2$ (Fig. S1) was 1614.15 (calculated, 1614.10). The ESI-MS (m/z) of CICA and HBPE, the ^{1}H NMR of HBPE and ^{13}C NMR characterization of HBPE-$CICA_6$ and HBPE-$CICA_2$ polymers were shown in ESI part (Fig. S2-S5).

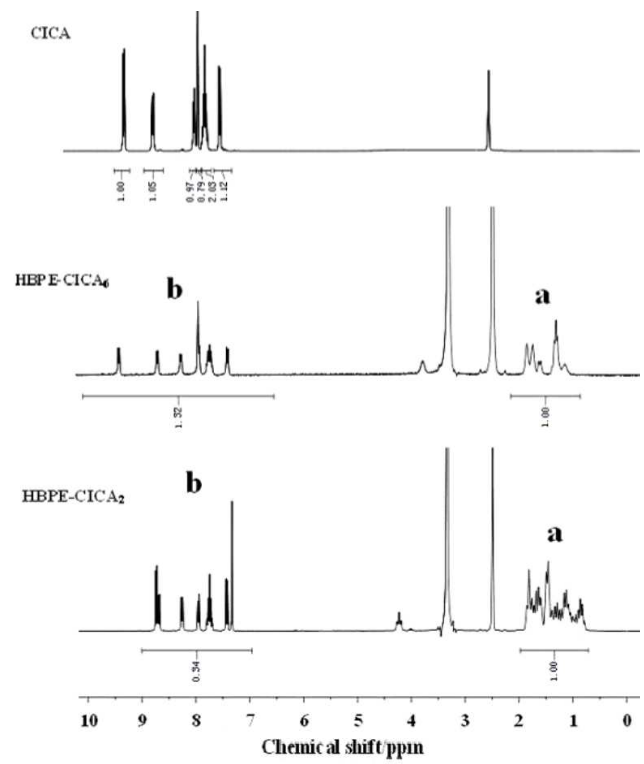

Fig. 2 ^{1}HNMR spectra of CICA and HBPE-$CICA_6$ and HBPE-$CICA_2$

Transmission electron microscope (TEM) experiments were performed to estimate the size and morphology of HBPE-$CICA_6$ and HBPE-$CICA_2$. As shown in Fig. 3A, HBPE-$CICA_6$ exhibited a nanorod morphology with an average diameter of 100 nm and length of 1 μm. The slight agglomeration between the nanorods could also be observed, which might be related to its higher grafting rate. As a comparison, Fig. 3B illustrated the TEM image of HBPE-$CICA_2$ with a nanorod morphology as well, while an average diameter of 200 nm and length of 1 μm. Additionally, HBPE-$CICA_2$ nanoparticles could self-assembly to form short nanorods with an average diameter of around 100 nm (Fig. 3C), and further assemble into long HBPE-$CICA_2$ nanorods (Fig. 3D). We suggest that the synergistic effect by hydrogen bonding in the flexible cores and π-π stacking interactions of peripheral CICA groups were responsible for the 1D molecular designs demonstrated here.[26,40,41] The 1D structures from intermolecular hydrogen bonds among hydroxy groups of the core and the π-π stacking interactions of peripheral CICA groups stacked in a face-to-face manner can be considered the primary cause for the formation of straight microrods (Fig. 3E). For the HBPE-$CICA_2$ showed the better nanorod morphology than that of the HBPE-$CICA_6$, its solution was stored at 4 °C for one month and it was observed that there was no change in size and morphology (Fig. S6). The results indicated that the HBPE-$CICA_2$ nanorods were very stable in ethyl acetate solution.

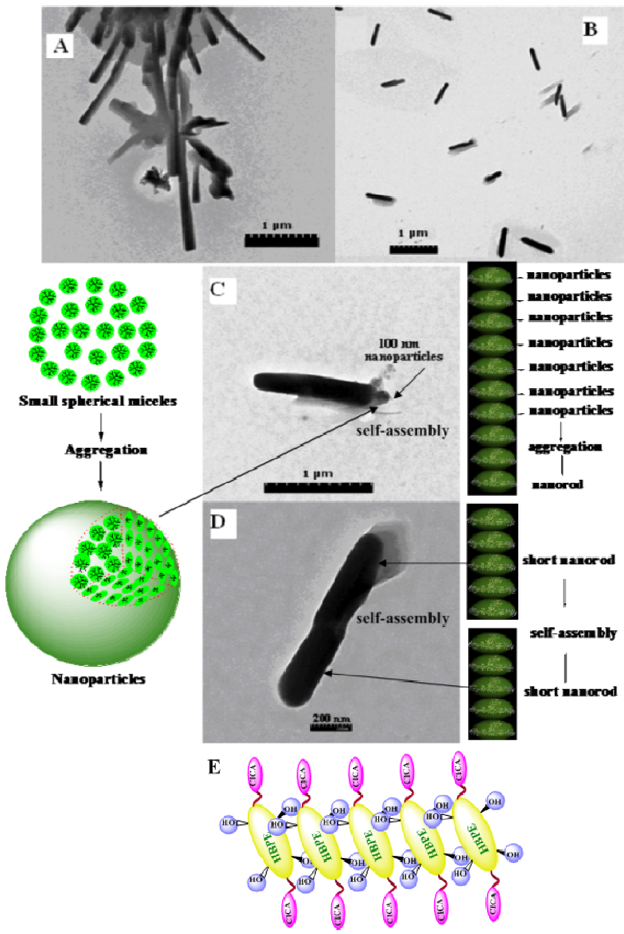

Fig. 3 (A) TEM images of HBPE-$CICA_6$ nanorods. (B) TEM images of HBPE-$CICA_2$ nanorods. (C) HBPE-$CICA_2$ nanorod obtained by the self-assemble of the nanoparticles. (D) Long HBPE-$CICA_2$ nanorod obtained by the self-assemble of the short nanorods. (E) Molecular models of possible conformations and assemblies of HBPE-$CICA_6$ or HBPE-$CICA_2$ nanorods. All the samples were used as stock solutions in ethyl acetate solution (0.010 mg/mL) after treated by ultrasonic (100 Hz) for 5 min, and stored at room temperature for 1 hour.

Atomic force microscopy (AFM) was also used to seen the surface morphology of these hyperbranched HBPE-$CICA_6$ and HBPE-$CICA_2$. The AFM of HBPE-$CICA_2$ was shown in Fig. 4, their top surface displayed a multilayered "onion-like" morphology[5, 24] (Fig. 4A). Fig. 4B was the magnified layer, the height of a single layer was approximately 4-5 nm, as shown in Fig.4C. The general morphology of the HBPE-$CICA_6$ is similar to that discussed above for HBPE-$CICA_2$.

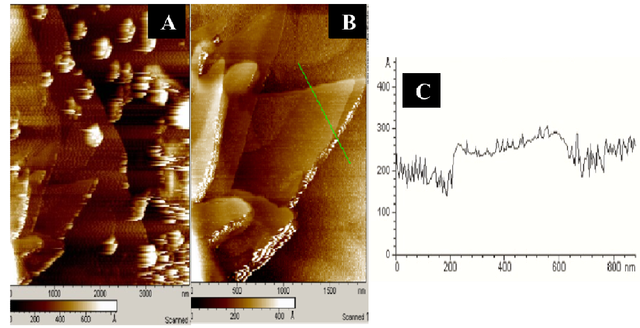

Fig. 4 Atomic force microscopy images of HBPE-$CICA_2$

X-ray diffraction data from the nanorods composed of HBPE-$CICA_6$ showed a series of sharp peaks that indicate a highly ordered crystalline structure in which the pyrrolo[2,1-a]isoquinoline terminal groups exihibit long-range order (Fig. 5, curve A). The strongest peak at 2θ = 18° corresponds to a d-spacing of 4.94 Å along the main axis of the pyrrolo[2,1-a]isoquinoline molecules[5]. The X-ray diffraction data from the nanorods composed of HBPE-$CICA_2$ also showed a series of more sharp peaks than HBPE-$CICA_6$ (Fig. 5, curve B), which also indicate a highly ordered crystalline structure in which the pyrrolo[2,1-a]isoquinoline terminal groups exhibit more longer-range order. The stongest peak at 2θ = 7.7° showed the longer d-spacing of 11.5 Å. Although HBPE-$CICA_6$ also showed a series sharp peaks at 2θ = 7.7°, its peaks were much weaker than that of HBPE-$CICA_2$, which suggested that the nanorods of HBPE-$CICA_2$ showed the more organized nanostructures than HBPE-$CICA_6$. These results were consistent with the results of TEM tests.

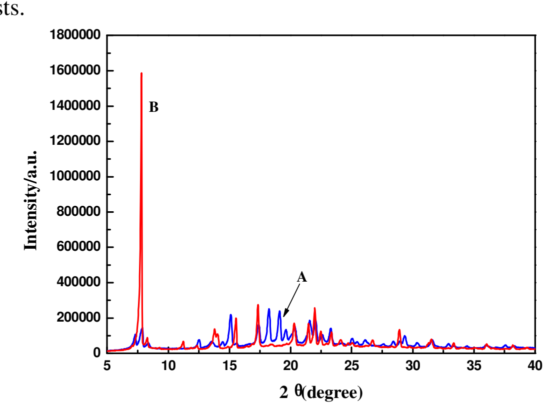

Fig. 5 X-ray diffraction data for nanorods formed from (A) HBPE-$CICA_6$ (blue line) and (B) HBPE-$CICA_2$ (red line)

For the π-π conjugate structure of the modified CICA groups, we examined the fluorescence of CICA, HBPE-$CICA_6$ and HBPE-$CICA_2$. Fluorescent spectra, digital camera image and fluorescent images of the CICA, HBPE-$CICA_6$ and HBPE-$CICA_2$ in DMSO solution were showed in Fig. 6, when the concentrations of the CICA, HBPE-$CICA_6$ and HBPE-$CICA_2$ solutions were same, the HBPE-$CICA_2$ nanorods showed the strongest fluorescent than HBPE-$CICA_6$ and CICA (order: HBPE-$CICA_2$ > HBPE-$CICA_6$ ≈ CICA), which was shown in digital camera images of Fig. 6.

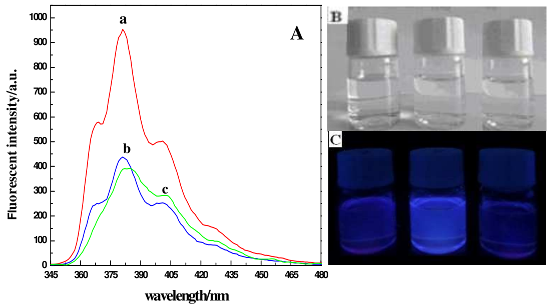

Fig. 6 (A) Fluorescence spectra of the HBPE-CICA$_2$ (a), HBPE-CICA$_6$ (b) nanorods and CICA (c) in DMSO solution (c = 5.0 × 10^{-5} M, λ_{ex}= 260 nm, the excitation and emission slits are 5nm/2.5nm). (B)The digital camera image of HBPE-CICA$_6$ (left) and HBPE-CICA$_2$ (middle) and CICA(right) in DMSO solution under sunlight. (C) The fluorescent image of HBPE-CICA$_6$ (left) and HBPE-CICA$_2$ (middle) and CICA(right) under UV light (λ= 260 nm), c = 5.0 × 10^{-5} M.

Iron is an ubiquitous metal in cells and plays a crucial role in a variety of vital cell functions,[42-45] However, both excess and deficiency from the normal permissible limit can induce serious disorders.[46, 47] Thus, there is an urgent need to develop chemical sensors that are capable of detecting the presence of iron ions in environmental and biological samples.

The influences of Fe^{3+} on the fluorescence intensity of the CICA, HBPE-CICA$_6$ and HBPE-CICA$_2$ have been evaluated by a fluorescence decreasement (FD = I/I_0) which is calculated by the ratio of the reduced fluorescence intensity in the presence of metal cations (I) and the fluorescence intensity without metal cations (I_0). The fluorescent responses of CICA, HBPE-CICA$_6$ and HBPE-CICA$_2$ to Fe^{3+} and other metal ions were shown in fluorescent part (Fig.S7-S11). The results indicated that they all showed better selectivities to Fe^{3+} than other metal ions. The fluorescent response of CICA and HBPE-CICA$_6$ to Fe^{3+} were shown in fluorescent part (Fig.S7-S10).

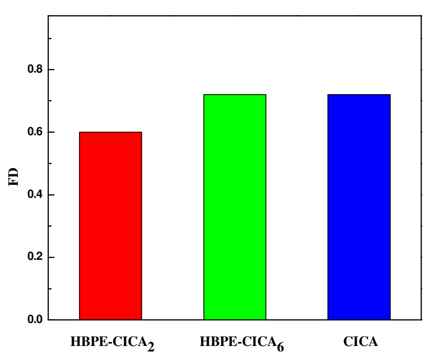

Fig. 7 Fluorescence decreasement factors (FD) of the HBPE-CICA$_2$, HBPE-CICA$_6$ and CICA（c = 5.0 × 10^{-5} M）in DMSO solution in the presence of Fe^{3+} at a concentration of 6.6× 10^{-5} M, λem = 380 nm.

When the concentration of CICA, HBPE-CICA$_6$ and HBPE-CICA$_2$ were same, HBPE-CICA$_2$ showed much stronger fluorescent, and in the case of the same concentration of Fe^3, HBPE-CICA$_2$ also showed the much less data of FD, which can be observed from Fig. 7. So we focused on the study of the fluorescent response of HBPE-CICA$_2$ to Fe^{3+}.

To further study the influence of grafting ratio of CICA on its sensitivity to the recognition of Fe^{3+}, the change of the fluorescent intensity of the HBPE-CICA$_6$ and HBPE-CICA$_2$ nanorods upon gradual titration with Fe^{3+} was carried out. As show in Fig. 8, when the concentration of the Fe^{3+} was maintained, the fluorescent decreasement factor (FD) of HBPE-CICA$_2$ was lower than that of HBPE-CICA$_6$. The relationship between the concentration of Fe^{3+} and FD was FD = 0.81-0.014 × [Fe^{3+}] for HBPE-CICA$_6$ and the fitting constant R= -0.9734, and for the HBPE-CICA$_2$, FD = 0.65-0.014× [Fe^{3+}], the fitting constant R= -0.9571, which showed that HBPE-CICA$_2$ with the lower grafting rate exhibited better sensitivity to Fe^{3+}, this might be the intermolecular hydrogen bonds among hydroxy groups of the flexible core and the π-π stacking interactions of peripheral CICA groups with the lower grafting rate could be easily destroyed by Fe^{3+}. As a result, in the process of design and synthesis, it's not need to graft more CICA binding units to the nanorods.

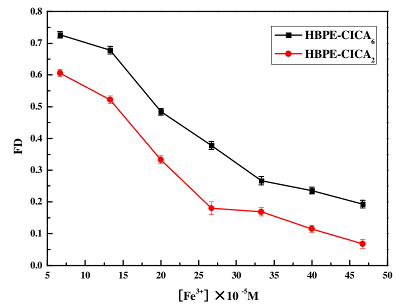

Fig. 8 Fluorescence decreasement factors (FD) of the HBPE-CICA$_6$（C = 5.0 × 10^{-5} M）and HBPE-CICA$_2$ （c = 5.0 × 10^{-5} M）nanorods in DMSO solution in the presence of Fe^{3+} at a concentration of 6.6× 10^{-5} M ~4.7 × 10^{-4} M, λem = 380 nm.

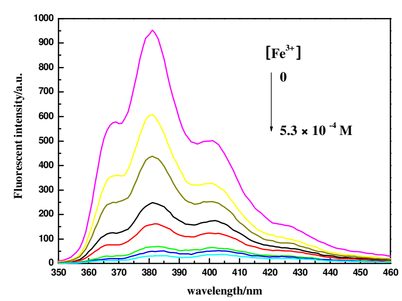

Fig. 9 Fluorescence spectra of the HBPE-CICA$_2$ nanorods in DMSO solution (C = 5.0 × 10^{-5} M, λex= 260 nm, the excitation and emission slit are 5nm/2.5nm) in the presence of Fe^{3+} at a concentration of 0~5.3 × 10^{-4} M.

The change of the fluorescence of the HBPE-CICA$_2$ nanorods upon gradual titration with Fe^{3+} was plotted in Fig. 9. The addition of Fe^{3+} caused a strong decrease in the fluorescent intensity and the greatest effect on FD had been observed at λ_{em}= 380 nm. As the fluorescence was very strong, the excitation and emission slits were adjusted to 5 nm/2.5 nm. The complex of the HBPE-CICA$_2$ nanorods with Fe^{3+} maybe trigger the mechanism of photoinduced electron transfer (PET) "OFF-ON" switching.[48] This is because, as usually observed, the electron transfer from the CN group to the excited state CICA moiety quenches the emission.

In summary, herein we reported a novel class of functionalized hyperbranched polyesters with CICA unit which were synthesized by a facile method under mild reaction condition. We found that the amplification of directional supramolecular interactions facilitated by the presence of multiple peripheral branches of even irregular, flexible molecules could lead to efficient self-assembly and form remarkably stable nanorods. The results demonstrated that one-dimensional supramolecular assembling could be achieved by highly branched but irregular molecules without a tedious, multistep synthesis of the well-defined, shape-persistent molecules. On the other hand, such hyperbranched aromatic-aliphatic polyesters exhibited strong fluorescent intensity, different grafting rate, nanorod morphology and good solubilities. Furthermore, HBPE-CICA$_6$ and HBPE-CICA$_2$ were established to be selective fluorescent sensor for Fe^{3+} ion detection since fluorescent responses of the functionalized HBPE were disparate to tested metal ions, in particular, lower grafted HBPE-CICA$_2$ nanorods showed better sensitivity to Fe^{3+} ion. The chelation formed between Fe^{3+} and the HBPE-CICA nanorods could be potentially applied for the design of new organic-inorganic hybrid materials.

.

Notes and references

1. *Jiangsu Key Laboratory of Biofunctional Materials，Key Laboratory of applied photochemisty, School of Chemistry and Materials Science, Nanjing Normal University, Nanjing 210097(China).*

2. *Jiangsu Provincial Key Laboratory of Biomass Energy and Materials, National Engineering Laboratory for Biomass Chemical Utilization, Institute of Chemical Industry of Forest Products, CAF, Nanjing 210042, (China).*

Fax:86 025 85891397; Tel:86 025 85891397; E-mail: wangbingxiang@njnu.edu.cn, hanqiaorong@njnu.edu.cn

† details of any supplementary information available should be included here

‡ Acknowledgements: We gratefully thank the financial support of the Priority Academic Program Development of Jiangsu Higher Education Institutions

1. H. B. Jin, Y. *L.* Zheng, Y. Liu, H. X. Cheng, Y. F. Zhou and D. Y. Yan, *Angew. Chem. Int. Ed*., 2011, **50**, 10352–10356.
2. N. E. Ikladious, J. N. Asaad and N. N. Rozik, *Des. Monomers Polym.*, 2009, **12**, 469–481.
3. H. B. Jin, W. Huang, Y. L. Zheng, Y. F. Zhou and D. Y. Yan, *Chem.-Eur. J*., 2012, **18**, 8641–8646.
4. T. W. Wang, M. J. Li, H. X. Gao and Y. Wu, *J. Colloid Interf. Sci.*, 2011, **353**, 107–115.
5. M. Ornatska, S. Peleshanko, B. Rybak, J. Holzmueller and V. V. Tsukruk, *Adv, Mater*., 2004, **16**, 23-24, 2206-2212.
6. J. Y. Liu, Y. Pang, W. Huang, X. H. Huang, L. L. Meng, X. Y. Zhu, Y. F. Zhou and D. Y. Yan, *Biomacromolecules*, 2011, **12** (5), 1567–1577.
7. Z. P. Guo, Y. H. Li, H. Y. Tian, X. L. Zhuang, X. S. Chen and X. B. Jing, *Langmuir*, 2009, **25** (17), 9690–9696.
8. Y. Liu, C.Y. Yu, H. B. Jin, B. B. Jiang, X.Y. Zhu, Y. F. Zhou, Z. Y. Lu and D. Y. Yan, *J. Am. Chem. Soc*., 2013, **135** (12), 4765–4770.
9. J. Y. Liu, W. Huang, Y. Pang, X. Y. Zhu, Y. F. Zhou and D. Y. Yan, *Langmuir*, 2010, **26** (13), 10585–10592.
10. S. Santra, C. Kaittanis and J. Manuel Perez, *Langmuir,* 2010, **26**, 5364–5373.
11. R. Reul, J. Nguyen and T. Kissel, *Biomaterials,* 2009, **30**, 5815–5824.
12. M. R. Rekha, C. P. Sharma, *Biomaterials* 2009, **30**, 6655–6664.
13. J. Y. Liu, Y. Pang, W. Huang, X. Y. Zhu, Y. F. Zhou and D. Y. Yan, *Biomaterials,* 2010, **31**, 1334–1341.
14. N. A. A. Rossi, I. Constantinescu, R. K. Kainthan, D. E. Brooks, M. D. Scott and J. N. Kizhakkedathu, *Biomaterials*, 2010, **31**, 4167–4178.
15. C. Mugabe, R. T. Liggins, D. Guan, I. Manisali, I. Chafeeva, D. E. Brooks, M. Heller, J. K. Jackson and H. M. Burt, *Int. J. Pharm*., 2011, **404**, 238–249.
16. Q. H. Miao, D. X. Xu, Z. Wang, L. Xu, T. W. Wang, Y. Wu, D. B. Lov6o, *Biomaterials*, 2010, **31**, 7364–7375.
17. J-F. Stumbe´ and B. Bruchmann, *Macromol. Rapid Commun*., 2004, **25**, 921–924.
18. X. Q. Yang, J. J. Grailer, S. Pilla, D. A. Steeber and S. Q. Gong, *Bioconjugate Chem*., 2010, **21**, 496–504.
19. S. Chen, X. Z. Zhang, S. X. Cheng, R. X. Zhuo and Z. W. Gu, *Biomacromolecules*, 2008, 9, 2578–2585.
20. R. J. Boohaker, G. Zhang, M. W. Lee, K. N. Nemec, S. Santra, J. M. Perez and A. R. Khaled, *Pharmaceutics*, 2012, **9**, 2080–2093.
21. S. Santra, C. Kaittanis and J. M. Perez, *Molecular Pharmaceutics*, 2010, 7(4), 1209–1222.
22. X. H. Wang, H. W. Liu, Y. Jin and C. H. Chen, *J. Phys. Chem. B*, 2006, **110**, 10236–10240.
23. Q. R. Han, X. H. Chen, Y. L. Niu, B. Zhao, B. X. Wang, C. Mao, L. B. Chen and J. Shen, *Langmuir*, 2013, **29**, 8402–8409.
24. M. Ornatska, S. Peleshanko, K. L. Genson, B. Rybak, K. N. Bergman and V. V. Tsukruk, *J. Am. Chem. Soc*., 2004, **126**, 9675-9684.
25. B. M. Rybak, M. Ornatska, K. N. Bergman, K. L. Genson and V. V. Tsukruk, *Langmuir* 2006, **22**, 1027-1037.
26. K. N. Bergman, B. M. Rybak, M. Ornatska and V. V. Tsukruk, *Polymer Preprints*, 2006, **47**(1), 591.
27. J. G. Kettle, S. Brown, C. Crafter, B. R. Davies, P. Dudley, G. Fairley, P. Faulder, S. Fillery, H. Greenwood, J. Hawkins, M. James, K. Johnson, C. D. Lane, M. Pass, J. H. Pink, H. Plant and S. C. Cosulich, *J. Med. Chem*., 2012, **55**, 1261–1273.
28. P. G. Baraldi, D. Preti, P. A. Borea and K. Varani, *J. Med. Chem*., 2012, **55**, 5676–5703.
29. F. Crestey, A. A. Jensen, M. Borch, J. T. Andreasen, J. Andersen, T. Balle and J. L. Kristensen, *J. Med. Chem*., 2013, **56**, 9673–9682.
30. E. Ahmed, A. L. Briseno, Y. M. Xia and S. A. Jenekhe, *J. Am. Chem. Soc*., 2008, **130**, 1118-1119.
31 P. P. Cui, L. Xu, Z. J. Shi and L. B. Gan, *J. Org. Chem*., 2011, **76**, 4210–4212.
32. M. Kucukdisli and T. Opatz, *J. Org. Chem*., 2013, **78**, 6670–6676.
33. H. Li, S. A. Bonderoff, B. Cheng and A. Padwa, *J. Org. Chem*., 2011, **76**, 4210–4212.
34. H. Q. Zhou, D. P. Danger, S. T. Dock, L. Hawley, S. G. Roller, C. D. Smith and A. L. Handlon, *ACS Med. Chem. Lett*., 2010, **1**, 19–23.
35. X. Wang, S.Y. Li, Y. M. Pan, H. S. Wang, H. Liang, Z. F. Chen and X. H. Qin, *Org. Lett*., 2014, **16**, 580–583.
36. A. K. Verma, R. R. Jha, R. Chaudhary, R. K. Tiwari, K. S. K. Reddy and A. Danodia, *J. Org. Chem*., 2012, **77**, 8191–8205.
37. C. H. Zhang, H. Zhang, L. Y. Zhang, T. B. Wen, X. M. He and H. P. Xia, *Organometallics*, 2013, **32**, 3738–3743.
38. L. H. Chung and C. Y. Wong, Organometallics, 2013, **32**, 3583–3586.
39. M. Kim, Y. Jung and I. Kim, *J. Org. Chem*., 2013, **78**, 10395–10404.
40. M. Zheng, H. Q. Tan, Z. G. Xie, L. G. Zhang, X. B. Jing and Z. C. Sun, Mater. Interfaces, 2013, **5**, 1078–1083.
41. M. Ornatska, K. N. Bergman, M. Goodman, S. Peleshanko, V. V. Shevchenko, V. V. Tsukruk, *Polymer*, 2006, **47**, 8137-8146.
42. C. X. Yang, H. B. Ren and X. P. Yan, *Anal. Chem*., 2013, **85**, 7441–7446.
43. R. Kagit, M. Yildirim, O. Ozay, S. Yesilot and H. Ozay, *Inorg. Chem*., 2014, **53**, 2144–2151.
44. D. P. Kennedy, C. D. Incarvito and S. C. Burdette, *Inorg. Chem*., 2010, **49**, 916–923.
45. T. Y. Cheng, Y. F. Xu, S. Y. Zhang, W. P. Zhu, X. H. Qian and L. P. Duan, *J. Am. Chem. Soc*., 2008, **130**, 16160–16161.
46. Z. Yang, M.Y. She,; B. Yin, J. H. Cui, Y. Z. Zhang, W. Sun, J. L. Li and Z. Shi, *J. Org. Chem.,* 2012, **77**, 1143–1147.
47. A. J. Weerasinghe, C. Schmiesing, S. Varaganti, G. Ramakrishna and

E. Sinn, *J. Phys. Chem. B*, 2010, **114**, 9413–9419.
48. G. J. Zhang, H. Y. Li, S. M. Bi, L. F. Song, Y. X. Lu, L. Zhang, J. J. Yu and L. M. Wang, *Analyst*, 2013, **138**, 6163–6170.

Graphical Abstract

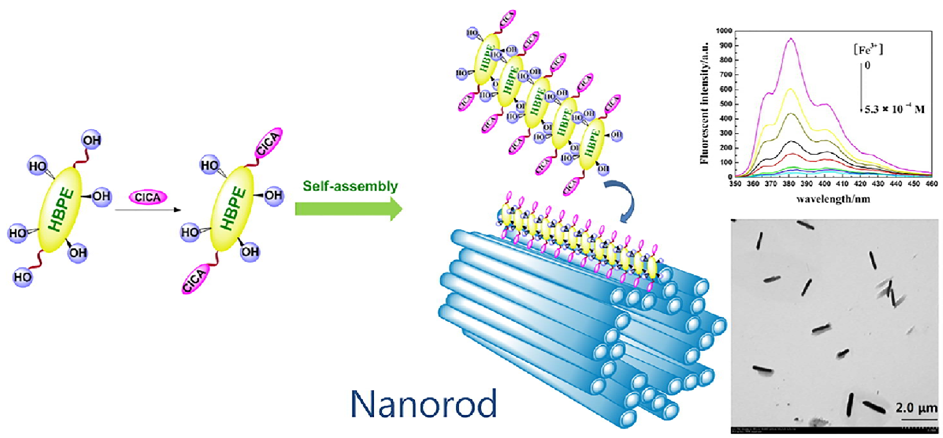

The novel functionalized hyperbranched aromatic-aliphatic co-polyester nanorods HBPE-$CICA_6$ and HBPE-$CICA_2$ were synthesized by a facile method under mild reaction conditions by modifing periphery of the second generation hyperbranched polyester (HBPE) with 1-cyano-pyrrolo[2,1-a]isoquinoline-3-carboxylic acid (CICA) groups. Such hyperbranched polyesters nanorods exhibited strong fluorescent intensity, different grafting rate, nanorod morphology and good solubilities. Interestingly, lower grafted HBPE-$CICA_2$ nanorods was established to be a highly sensitive fluorescent sensor for Fe^{3+} ion.